DOI: http://dx.doi.org/10.12989/sem.2005.19.4.381

Piecewise exact solution for analysis of base-isolated structures under earthquakes

C. S. Tsai†

Department of Civil Engineering, Feng Chia University, Taichung, Taiwan 407, R.O.C.

Tsu-Cheng Chiang‡

Graduate Institute of Civil and Hydraulic Engineering, Feng Chia University, Taichung, Taiwan 407, R.O.C.

Bo-Jen Chen‡†

R&D Department, Earthquake Proof System, Inc, Taichung, Taiwan 404, R.O.C.

Kuei-Chi Chen‡‡

Graduate Institute of Civil and Hydraulic Engineering, Feng Chia University, Taichung, Taiwan 407, R.O.C.

(Received September 26, 2003, Accepted November 3, 2004)

Abstract. Base isolation technologies have been proven to be very efficient in protecting structures from seismic hazards during experimental and theoretical studies. In recent years, there have been more and more engineering applications using base isolators to upgrade the seismic resistibility of structures. Optimum design of the base isolator can lessen the undesirable seismic hazard with the most efficiency. Hence, tracing the nonlinear behavior of the base isolator with good accuracy is important in the engineering profession. In order to predict the nonlinear behavior of base isolated structures precisely, hundreds even thousands of degrees-of-freedom and iterative algorithm are required for nonlinear time history analysis. In view of this, a simple and feasible exact formulation without any iteration has been proposed in this study to calculate the seismic responses of structures with base isolators. Comparison between the experimental results from shaking table tests conducted at National Center for Research on Earthquake Engineering in Taiwan and the analytical results show that the proposed method can accurately simulate the seismic behavior of base isolated structures with elastomeric bearings. Furthermore, it is also shown that the proposed method can predict the nonlinear behavior of the VCFPS isolated structure with accuracy as compared to that from the nonlinear finite element program. Therefore, the proposed concept can be used as a simple and practical tool for engineering professions for designing the elastomeric bearing as well as sliding bearing.

Key words: exact solution; rubber bearing; friction pendulum system; base isolation; structural control; seismic engineering.

---

† Professor, Corresponding author, E-mail: cstsai@fcu.edu.tw
‡ Ph. D.
‡†Ph. D., Research Assistant Fellow
‡‡ Ph. D. Candidate

1. Introduction

Structures and their internal contents can be protected during severe earthquake events with the installation of base isolators. The seismic response of the superstructure can be mitigated within a desirable range by using the method of shifting the fundamental frequency of the conventional fixed-base structure away from the predominant frequencies of ground excitations. In recent years, a number of base isolators have been proposed and the effectiveness of each in mitigating the seismic response of a structure has been investigated through theoretical and experimental studies. In general, the base isolator can be classified into two groups: the elastomeric and sliding type base isolators. The Stirrup Rubber Bearing (SRB) (Tsai *et al.* 2002, 2003a, Chen 2003), which belongs to the elastomeric bearing, and the Variable Curvature Friction Pendulum System (VCFPS) (Tsai *et al*. 2003b), which belongs to the sliding bearing, have been adopted in this study.

In the past, different numerical algorithms with different mathematical models for a multiple degree-of-freedom base-isolated structure have been proposed. Due to the highly nonlinear behavior of the base isolator, the step-by-step time history algorithm is the fundamental requisition for the calculation of the seismic response of a multiple degree-of-freedom base isolated structure. In order to provide a simple tool for engineering professions to design the elastomeric and sliding bearings without any inconvenience during preliminary design. Exact solutions considering superstructure as a rigid body for base isolated structure with elastomeric-type isolators and sliding-type isolators have been proposed. The concept of the piecewise exact method for a linear system proposed by Nigam and Jennings (1968, 1969) has been further extended to the nonlinear hysteretic analysis of the base-isolated structure during earthquake ground motions. Very good agreement can be observed obviously from the comparison between exact solutions and experimental results of shaking table tests using SRB isolators. It is also revealed that the exact solutions are very close to the numerical results calculated from finite element computer program (Tsai 1996).

2. Mechanical behavior for elastomeric isolator

The Wen's model in an incremental form has been proposed by Tsai *et al*. (2003c). The increment of the horizontal force of the base isolator can be expressed as:

$$dF(\tau) = \alpha\frac{F_y}{Y}dx_b(\tau) + (1-\alpha)F_y dZ(\tau) \tag{1}$$

where F_y and Y represent the yield force and yield displacement, respectively; $dx_b(\tau)$ is the increment of the horizontal displacement; $dZ(\tau)$ denotes the increment of dimensionless parameter that controls the plastic behaviour of the elastomeric bearing; α is the ratio of the post-yielding stiffness to the elastic stiffness.

The ratio α can be represented as:

$$\alpha = \frac{k_p(x_b)}{k_e(x_b)} \tag{2}$$

where $k_p(x_b)$ is the post-yielding stiffness and $k_e(x_b)$ is the elastic stiffness.

The parameter $dZ(\tau)$ can be shown in the following form:

$$dZ(\tau) = \frac{A}{Y}dx_b(\tau) - \frac{Z^2(\tau)[\gamma\,\mathrm{sgn}(dx_b(\tau)\cdot Z(\tau)) + \beta]}{Y}dx_b(\tau) \tag{3}$$

Constantinou *et al.* (1990) have proposed that $A/(\beta+\gamma) = 1$. In particular, $A = 1$, $\beta = 0.1$ and $\gamma = 0.9$ are suggested.

One can set

$$Q(\tau) = \gamma\,\mathrm{sgn}(dx_b(\tau)\cdot Z(\tau)) + \beta \tag{4}$$

Thus, Eq. (3) can be rewritten as:

$$dZ(\tau) = \frac{1}{Y}(A - Z^2(\tau)\cdot Q(\tau))dx_b(\tau) \tag{5}$$

Backsubstitution of Eq. (5) into Eq. (1) gives:

$$dF(\tau) = \frac{F_y}{Y}[\alpha + (1-\alpha)\cdot(A - Z^2(\tau)\cdot Q(\tau))]dx_b(\tau) \tag{6}$$

The horizontal stiffness of the elastomeric bearing can be obtained from Eq. (6) as:

$$k_b(x_b) = \frac{F_y}{Y}[\alpha + (1-\alpha)\cdot(A - Z^2(\tau)\cdot Q(\tau))] \tag{7}$$

Therefore, the isolation frequency of a base-isolated structure using elastomeric bearings can be given as:

$$\omega_n^2(x_b) = \frac{k_b(x_b)}{m} = \frac{\frac{F_y}{Y}[\alpha + (1-\alpha)\cdot(A - Z^2(\tau)\cdot Q(\tau))]}{m} \tag{8}$$

3. Piecewise exact solution for base isolated structure using elastomeric bearings

As shown in Fig. 1, the time history of the ground acceleration is composed of piecewise linear segments; namely, the time history of the ground motion between time t_{i-1} and t_i can be reasonably assumed as a linear variation (Chopra 1995). As shown in Fig. 2, if the superstructure moves as a rigid body and the first mode of the base-isolated structure involves deformation only in the isolation system under earthquakes, the isolated structure can be idealized as a SDOF system. Then, the equation of motion of the base isolated structure can be given by:

$$m\ddot{x}_b + c_b\dot{x}_b + k_b(x_b)x_b = -m\ddot{x}_g^{i-1} - \frac{m\ddot{x}_g^{i} - m\ddot{x}_g^{i-1}}{\Delta t}\tau \tag{9}$$

where m, c_b and $k_b(x_b)$ are the total mass of the base isolated structure, damping coefficient and horizontal stiffness of the base isolator, respectively; x_b is the horizontal displacement of the base isolator relative to the ground; and $\ddot{x}_g^{i}$ is the ground acceleration at time t_i.

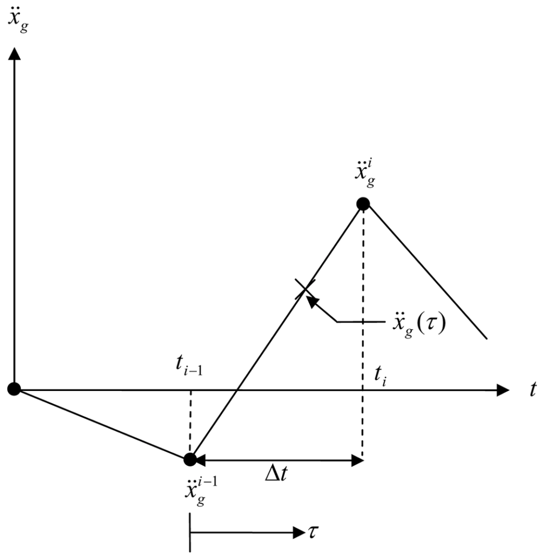

Fig. 1 Linear interpolation for ground motions

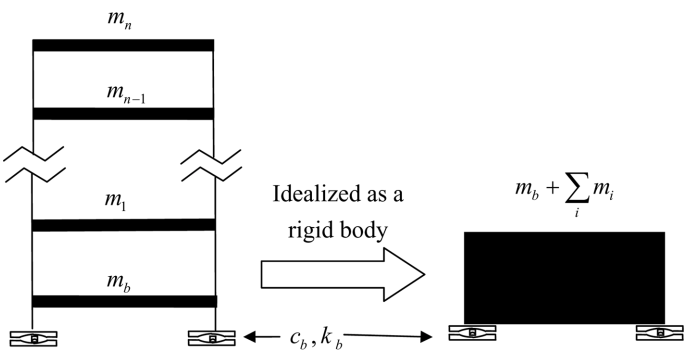

Fig. 2 Idealization of rigid body motion for superstructure

The displacement response consisting of the free-vibration response and the particular solution between time t_{i-1} and time t_i is obtained as:

$$x_b(\tau) = (C\cos\omega_d\tau + D\sin\omega_d\tau)\exp(-\xi\omega_n\tau) + \frac{1}{\omega_n^2}\left[-\ddot{x}_g^{i-1} + \frac{2\xi}{\omega_n\Delta t}(\ddot{x}_g^{i} - \ddot{x}_g^{i-1})\right] - \left(\frac{\ddot{x}_g^{i} - \ddot{x}_g^{i-1}}{\omega_n^2\Delta t}\right)\tau \tag{10}$$

where ξ is the viscous damping ratio.

In the beginning of each time step, the isolator displacement is equal to that at the end of the previous time step, $x_b(0) = x_b^{i-1}$, then:

$$C = x_b^{i-1} - \frac{1}{\omega_n^2}\left[-\ddot{x}_g^{i-1} + \frac{2\xi}{\omega_n\Delta t}(\ddot{x}_g^{i} - \ddot{x}_g^{i-1})\right] \tag{11}$$

The velocity response can be obtained form Eq. (10) as:

$$\begin{aligned}\dot{x}_b(\tau) &= (-\omega_d C\sin\omega_d\tau + \omega_d D\cos\omega_d\tau)\exp(-\xi\omega_n\tau)\\ &-\xi\omega_n(C\cos\omega_d\tau + D\sin\omega_d\tau)\exp(-\xi\omega_n\tau)\\ &-\left(\frac{\ddot{x}_g^i - \ddot{x}_g^{i-1}}{\omega_n^2\Delta t}\right)\end{aligned} \tag{12}$$

In the beginning of each time step, the velocity is equal to that at the end of the previous time step, $\dot{x}_b(0) = \dot{x}_b^{i-1}$, thus:

$$D = \frac{\dot{x}_b^{i-1}}{\omega_d} + \frac{\xi}{\sqrt{1-\xi^2}}x_b^{i-1} - \frac{\xi}{\omega_n^2\sqrt{1-\xi^2}}\left[-\ddot{x}_g^{i-1} + \frac{2\xi}{\omega_n\Delta t}(\ddot{x}_g^i - \ddot{x}_g^{i-1})\right] + \left(\frac{\ddot{x}_g^i - \ddot{x}_g^{i-1}}{\omega_d\omega_n^2\Delta t}\right) \tag{13}$$

The derivative of the velocity with respect to time leads to the acceleration:

$$\begin{aligned}\ddot{x}_b(\tau) &= (-\omega_d^2 C\cos\omega_d\tau - \omega_d^2 D\sin\omega_d\tau)\exp(-\xi\omega_n\tau)\\ &-2\xi\omega_n(-\omega_d C\sin\omega_d\tau + \omega_d D\cos\omega_d\tau)\exp(-\xi\omega_n\tau)\\ &+\xi^2\omega_n^2(C\cos\omega_d\tau + D\sin\omega_d\tau)\exp(-\xi\omega_n\tau)\end{aligned} \tag{14}$$

4. Geometric formulation and mechanical behavior for VCFPS isolator

The mechanical behavior of VCFPS is very similar to that of the FPS proposed by Zayas (Zayas *et al.* 1987, Al-Hussaini *et al.* 1994). The difference between the VCFPS and FPS is that the radii of curvature of the VCFPS can be lengthened with an increase of the isolator displacement. Hence, the fundamental period of the base-isolated structure can be shifted further away from the predominant periods of near-fault ground motions, and the resonant possibility of the superstructure with earthquakes can be prevented.

As shown in Fig. 3, the geometric function used to describe the VCFPS base isolator can be expressed in the following (Tsai *et al.* 2003b):

$$y = R - \sqrt{R^2 - x_b^2} - f(x_b) \tag{15}$$

where R is the radius of curvature at the center of the sliding surface of the VCFPS; x_b is the horizontal displacement of the isolator; $f(x_b)$ is the function to describe the increase of the radius of curvature with an increase of the horizontal displacement.

If the function $f(x_b)$ is given as:

$$f(x_b) = E\,\mathrm{sgn}(x_b)x_b^3 \tag{16}$$

E is the parameter that describes the variation of curvature of the concave surface.

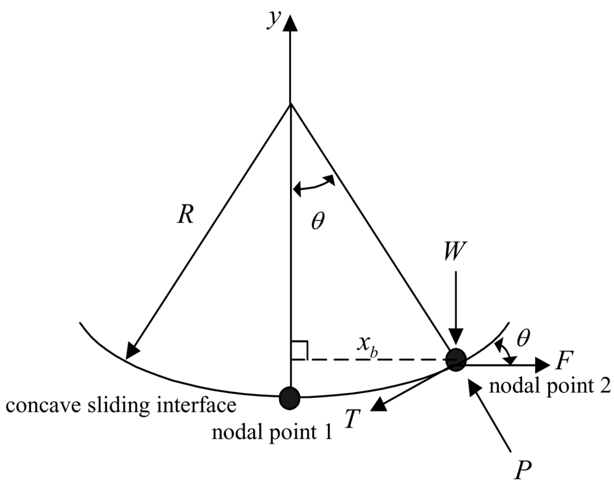

Fig. 3 Forces acting on concave sliding surface

Backsubstitution of Eq. (16) into Eq. (15) results in:

$$y = R - \sqrt{R^2 - x_b^2} - E\,\mathrm{sgn}(x_b)x_b^3 \tag{17}$$

As shown in Fig. 3, the equilibrium of VCFPS in vertical and horizontal directions can be shown as:

$$W - P\cos\theta + T\sin\theta = 0 \tag{18}$$

and

$$F - P\sin\theta - T\cos\theta = 0 \tag{19}$$

where W is the vertical loading; P denotes the reaction force normal to the concave surface; T is the friction force tangent to the concave surface; and F is the horizontal force imposing at the concave sliding surface.

Rearrangement of Eqs. (18) and (19) leads to:

$$F = W\tan\theta + \frac{T}{\cos\theta} = W\frac{dy}{dx_b} + \frac{T}{\cos\theta} \tag{20}$$

The slope of the concave sliding surface of the VCFPS can be obtained from Eq. (17) as:

$$\frac{dy}{dx_b} = \frac{x_b}{\sqrt{R^2 - x_b^2}} - 3E\,\mathrm{sgn}(x_b)x_b^2 \tag{21}$$

Backsubstitution of Eq. (21) into Eq. (20) yields:

$$F = W\left[\frac{x_b}{\sqrt{R^2 - x_b^2}} - 3E\,\mathrm{sgn}(x_b)x_b^2\right] + \frac{T}{\cos\theta} \tag{22}$$

If the restoring force can bring the slider back to the initial position within the sliding displacement x_0, then the parameter E can be determined as:

$$E = \frac{\dfrac{Wx_0}{\sqrt{R^2 - x_0^2}} - \dfrac{T_0}{\cos\theta_0}}{3W\mathrm{sgn}(x_0)x_0^2} \tag{23}$$

where T_0 is the static friction force.

Backsubstitution of Eq. (23) into Eq. (22) gives:

$$F = \left[\frac{W}{\sqrt{R^2 - x_b^2}} - \frac{\mathrm{sgn}(x_b)x_b\left(\dfrac{Wx_0}{\sqrt{R^2 - x_0^2}} - \dfrac{T_0}{\cos\theta_0}\right)}{\mathrm{sgn}(x_0)x_0^2}\right]x_b + \frac{T}{\cos\theta} = \bar{K}(x_b)x_b + \frac{T}{\cos\theta} \tag{24}$$

where $\bar{K}(x_b)$ represents the horizontal stiffness of the VCFPS and can be expressed as:

$$\bar{K}(x_b) = \frac{W}{\sqrt{R^2 - x_b^2}} - \frac{\mathrm{sgn}(x_b)x_b\left(\dfrac{Wx_0}{\sqrt{R^2 - x_0^2}} - \dfrac{T_0}{\cos\theta_0}\right)}{\mathrm{sgn}(x_0)x_0^2} \tag{25}$$

If the variation of the vertical loading due to the overturning moment is neglected, then the isolation frequency of VCFPS isolated structure can be obtained as:

$$\omega_n^2 = \frac{g}{\sqrt{R^2 - x_b^2}} - \frac{\mathrm{sgn}(x_b)x_b\left(\dfrac{gx_0}{\sqrt{R^2 - x_0^2}} - \dfrac{\mu_{\min}g}{\cos\theta_0}\right)}{\mathrm{sgn}(x_0)x_0^2} \tag{26}$$

where $\mu_{\min}$ is the friction coefficient at zero sliding velocity. It should be noted from Eq. (26) that the isolation frequency is a function of the horizontal displacement rather than a constant value.

5. Piecewise exact solution for VCFPS isolated structure

Based on the concept of idealizing the superstructure as a rigid body under earthquakes, the equation of motion of a base isolated structure considering the superstructure as a rigid body can be expressed as:

$$m\ddot{x}_b + c_b\dot{x}_b + k_b(x_b)x_b = -\mu(\dot{x}_b)mg\mathrm{sgn}(\dot{x}_b) - m\ddot{x}_g^{i-1} - \frac{m\ddot{x}_g^{i} - m\ddot{x}_g^{i-1}}{\Delta t}\tau \tag{27}$$

where m, c_b and $k_b(x_b)$ are the total mass of the base isolated structure, damping coefficient and horizontal stiffness of the base isolator, respectively; x_b is the horizontal displacement of the base isolator relative to the ground; $\mu(\dot{x}_b)$ is the friction coefficient of the sliding surface; and $\ddot{x}_g^i$ is the ground acceleration at time t_i.

The friction coefficient $\mu(\dot{x}_b)$ proposed by Al-Hussaini *et al.* (1994) can be shown in the following:

$$\mu(\dot{x}_b) = \mu_{\max} - (\mu_{\max} - \mu_{\min})\exp(-\alpha|\dot{x}_b|) \tag{28}$$

where $\mu_{\min}$ and $\mu_{\max}$ are the friction coefficients at zero sliding velocity and high sliding velocity, respectively; α is the parameter which controls the variation of friction with velocity.

Tsai (1995, 1997) also proposed an analytical model for the friction force which considers the variation of the friction force due to the instantaneous applied normal load P, sliding velocity V and energy accumulation in the sliding history:

$$F_t = \frac{PA^*}{\lambda_1 A^* + \lambda_2 P} \cdot \{1 + \beta_1[1 - \exp(-\beta_2 V)]\} \times Coef \tag{29}$$

where A^* represents the contact area at the interface; λ_1 and λ_2 are the parameters associated with the quasi static friction force; β_1 and β_2 are the parameters which control the variation of friction with velocity; *Coef* is a decay function which depicts the phenomenon of degradation of the friction force with the increase of the number of cyclic reversals. The coefficient of *Coef* can be given as:

$$Coef = (1 - \gamma_1) + \gamma_1 \cdot \exp\left(-\gamma_2 \cdot \int_0^t \frac{F_t - F_t^0}{F_t^0} \cdot d\bar{u}_T\right) \tag{30}$$

where γ_1 and γ_2 are parameters to describe the decay behavior of the friction force at the Teflon interface associated with the energy accumulation in the sliding history; F_t^0 is the friction force when the sliding velocity is equal to zero.

The transient solution of Eq. (27), $x_c(\tau)$ can be given as:

$$x_c(\tau) = (C\cos\omega_d\tau + D\sin\omega_d\tau)\exp(-\xi\omega_n\tau) \tag{31}$$

where ω_n is the natural frequency which is a function of the horizontal sliding displacement mentioned above; $\omega_d = \omega_n\sqrt{1-\xi^2}$ is the damped frequency; ξ is the viscous damping ratio.

The steady-state solution, $x_p(\tau)$ between time t_{i-1} and t_i is:

$$x_p(\tau) = \frac{1}{\omega_n^2}\left[-\mu(\dot{x}_b)g\,\mathrm{sgn}(\dot{x}_b) - \ddot{x}_g^{i-1} + \frac{2\xi}{\omega_n\Delta t}(\ddot{x}_g^i - \ddot{x}_g^{i-1})\right] - \frac{\ddot{x}_g^i - \ddot{x}_g^{i-1}}{\omega_n^2\Delta t}\tau \tag{32}$$

The sliding displacement of the base isolator between time t_{i-1} and t_i can be obtained from Eqs. (31) and (32) as:

$$\begin{aligned} x_b(\tau) &= (C\cos\omega_d\tau + D\sin\omega_d\tau)\exp(-\xi\omega_n\tau) \\ &+ \frac{1}{\omega_n^2}\left[-\mu(\dot{x}_b)g\,\mathrm{sgn}(\dot{x}_b) - \ddot{x}_g^{i-1} + \frac{2\xi}{\omega_n\Delta t}(\ddot{x}_g^i - \ddot{x}_g^{i-1})\right] - \frac{\ddot{x}_g^i - \ddot{x}_g^{i-1}}{\omega_n^2\Delta t}\tau \end{aligned} \tag{33}$$

In the beginning of each time step, the sliding displacement is equal to that at the end of the previous time step, $x_b(0) = x_b^{i-1}$, thus, the coefficient C can be obtained as:

$$C = x_b^{i-1} - \frac{1}{\omega_n^2}\left[-\mu(\dot{x}_b)g\,\mathrm{sgn}(\dot{x}_b) - \ddot{x}_g^{i-1} + \frac{2\xi}{\omega_n \Delta t}(\ddot{x}_g^i - \ddot{x}_g^{i-1})\right] \tag{34}$$

If the friction coefficient is assumed approximately constant in the time step, the derivative of Eq. (33) respect to τ yields:

$$\begin{aligned}\dot{x}_b(\tau) &= (-\omega_d C\sin\omega_d\tau + \omega_d D\cos\omega_d\tau)\exp(-\xi\omega_n\tau)\\ &- \xi\omega_n(C\cos\omega_d\tau + D\sin\omega_d\tau)\exp(-\xi\omega_n\tau) - \frac{\ddot{x}_g^i - \ddot{x}_g^{i-1}}{\omega_n^2\Delta t}\end{aligned} \tag{35}$$

In the beginning of each time step, the velocity is equal to that at the end of the previous time step, $\dot{x}_b(0) = \dot{x}_b^{i-1}$, thus, the coefficient D can be obtained as:

$$D = \frac{1}{\omega_d}\left\{\dot{x}_b^{i-1} + \xi\omega_n x_b^{i-1} - \frac{\xi}{\omega_n}\left[-\mu(\dot{x}_b)g\,\mathrm{sgn}(\dot{x}_b) - \ddot{x}_g^{i-1} + \frac{2\xi}{\omega_n\Delta t}(\ddot{x}_g^i - \ddot{x}_g^{i-1})\right] + \frac{\ddot{x}_g^i - \ddot{x}_g^{i-1}}{\omega_n^2\Delta t}\right\} \tag{36}$$

The sliding acceleration can be given as:

$$\begin{aligned}\ddot{x}_b(\tau) &= (-\omega_d^2 C\cos\omega_d\tau - \omega_d^2 D\sin\omega_d\tau)\exp(-\xi\omega_n\tau)\\ &-2\xi\omega_n(-\omega_d C\sin\omega_d\tau + \omega_d D\cos\omega_d\tau)\exp(-\xi\omega_n\tau)\\ &+ \xi^2\omega_n^2(C\cos\omega_d\tau + D\sin\omega_d\tau)\exp(-\xi\omega_n\tau)\end{aligned} \tag{37}$$

Hence, the sliding displacement, sliding velocity and sliding acceleration can be obtained from Eqs. (33), (35) and (37), respectively.

5.1 Nonsliding phase

The summation of the inertial and restoring forces imposing at the base raft is lower than the static friction force, i.e.,:

$$|m(\ddot{x}_b + \ddot{x}_g) + k_b x_b| < \mu_{\min} mg \tag{38}$$

Then the structure will behave as a conventional fixed base structure, and the sliding displacement, sliding velocity and sliding acceleration are:

$$x_b = \text{constant}, \quad \dot{x}_b = \ddot{x}_b = 0 \tag{39}$$

5.2 Initiation of sliding phase

The base isolated structure will behave as a fixed base structure unless the static friction force can be overcome. During the sliding phase, the equation given in the following should be satisfied:

$$|m(\ddot{x}_b + \ddot{x}_g) + k_b x_b| \ge \mu_{\min} mg \tag{40}$$

Due to the time increment adopted in the time history analysis (e.g., $\Delta t = 0.0005$ sec) is much smaller than that of the sampling time interval of the earthquake history, it is reasonable to set that the direction of sliding at the current time step is the same as the previous time step. It should be noted that the direction of sliding remains unchanged during a particular sliding phase. At the end of each time step, the validity of inequality of Eq. (40) should be checked. If the inequality is not satisfied at a particular time step, then the structure enters a nonsliding phase and behaves as a fixed base structure.

6. Comparisons between exact solutions and experimental results for base isolated structure using SRB isolators

In order to verify the feasibility of the proposed method, the shaking table tests of a full scale steel structure with Stirrup Rubber Bearings were performed at the National Center for Research on Earthquake Engineering in Taiwan. As shown in Fig. 4, the three-story structure is 9 m in height and the total weight of the structure is about 40 tons. The properties of columns and girders of the steel structure are $H200 \times 200 \times 8 \times 12$ and $H200 \times 150 \times 6 \times 9$, respectively. The fundamental periods of the fixed-base structure in its longitudinal and transverse directions are 0.942 and 0.699 sec, respectively. In order to increase the rigidity of the superstructure, diagonal steel bracings ($2L100 \times 100 \times 13$) were installed on the structure during the tests. As shown in Fig. 5, the fundamental frequency of the fixed-base structure with diagonal bracings is 4.243 Hz (i.e., 0.236 sec in period) based on the experimental results of the white noise test of 0.05 g in PGA. The adopted SRB isolators shown in Fig. 6 adopted in this study are 200 mm in diameter and 104 mm height.

Fig. 4 Base-isolated structure with bracings on shaking table at the National Center for Research on Earthquake Engineering in Taiwan

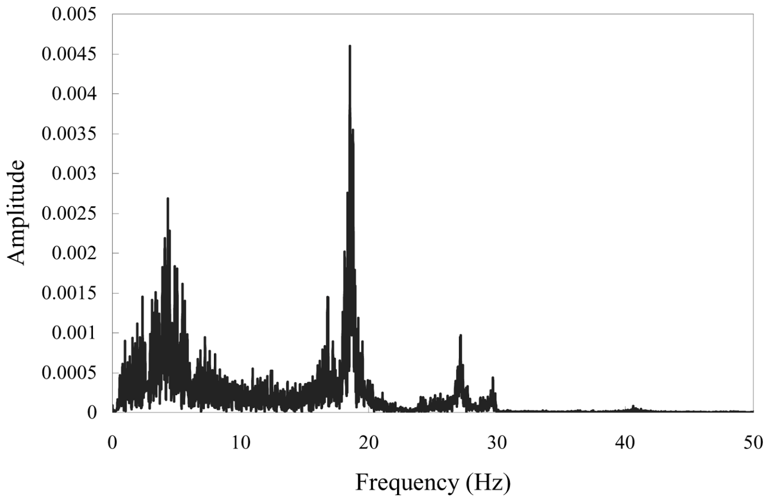

Fig. 5 Transfer function of roof acceleration of fixed-base structure under white noise test of 0.05 g in PGA

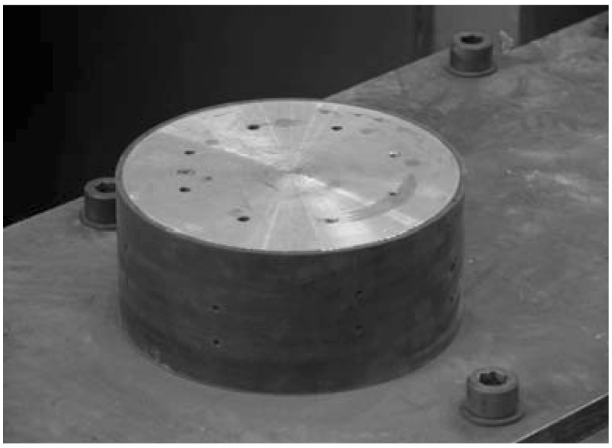

Fig. 6 The stirrup rubber bearing

The transfer function of the horizontal displacement of the SRB shown in Fig. 7 indicates that the installation SRB isolators can shift the fundamental period away from the predominant periods of earthquake excitations. Hence, it is reasonable to regard the superstructure of the base isolated structure as a rigid body during earthquakes.

The dimensionless parameters of α, A, β, γ for Eqs. (4) and (6) are 0.25, 1.0, 0.1, 0.9 and the yield displacement Y is 0.68 mm, respectively. The comparisons of the bearing displacement, bearing acceleration and hysteresis loop between the exact solution and the shaking table test during the 1940 El Centro earthquake of 0.116 g in PGA is presented from Fig. 8 to Fig. 10, respectively. Very good agreement between exact solutions and experimental results can be observed from these three figures. Therefore, the nonlinear behavior of the SRB isolator during earthquakes can be obtained by using the proposed method. During the shaking table tests, the SRB isolated structure subjected to the Chi-Chi earthquake (TCU129 station) was also performed. The displacement and

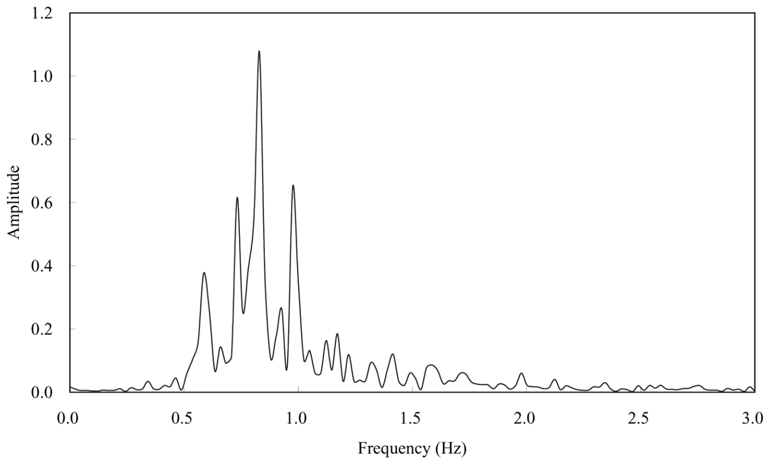

Fig. 7 Transfer function of relative displacement of SRB bearing under white noise test of 0.05 g in PGA

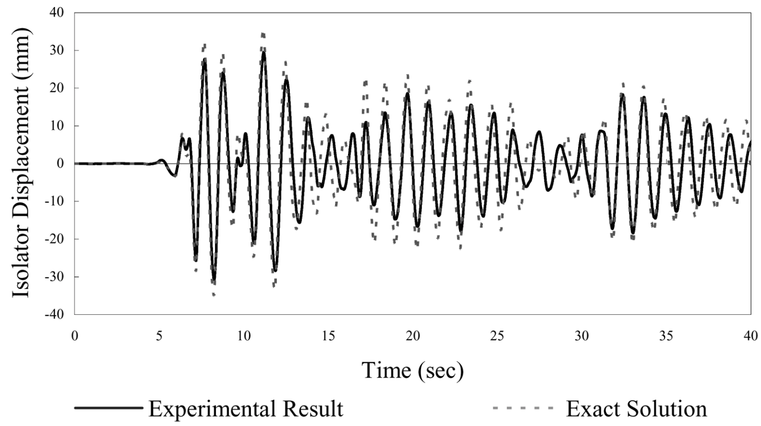

Fig. 8 Comparison of bearing displacement between exact solution and experimental results under El Centro earthquake of 0.116 g in PGA

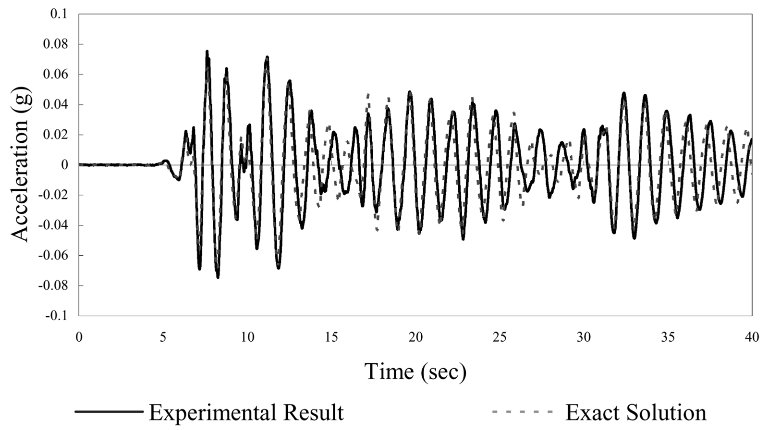

Fig. 9 Comparison of bearing acceleration between exact solution and experimental result under El Centro earthquake of 0.116 g in PGA

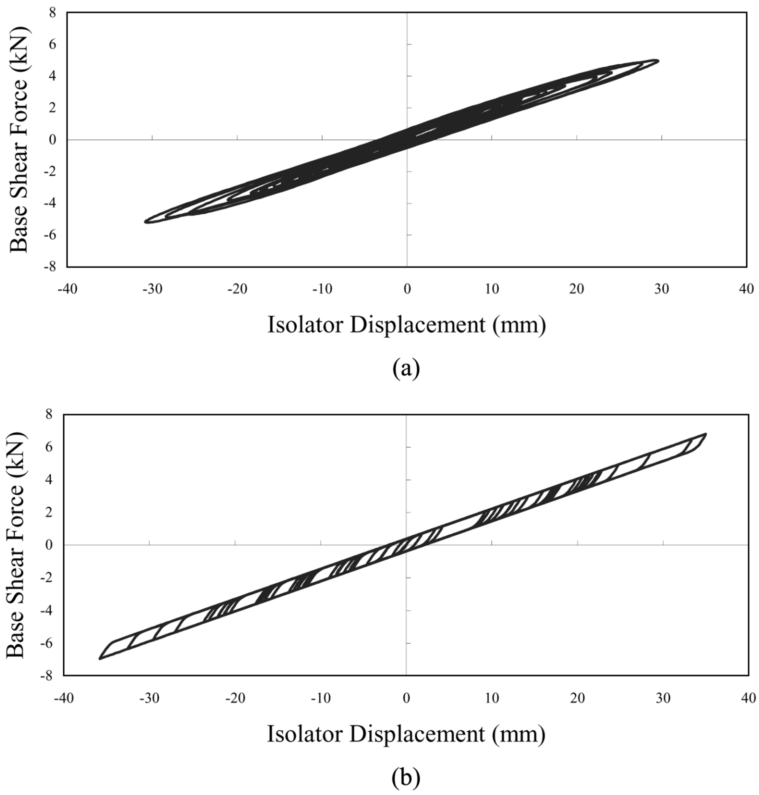

Fig. 10 Comparison of hysteresis loop between exact solution and experimental result under El Centro earthquake of 0.116 g in PGA: (a) Experimental result; (b) Exact solution

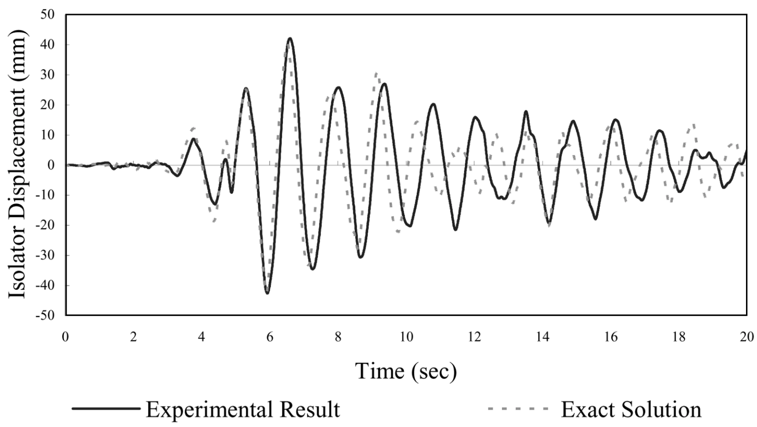

Fig. 11 Comparison of bearing displacement between exact solution and experimental result under Chi-Chi earthquake (TCU129) of 0.289 g in PGA

acceleration histories of the SRB isolator shown in Figs. 11 and 12 illustrate that exact solutions are very close to experimental results. Furthermore, it is also shown from Fig. 13 that the proposed method can trace the force-displacement loop with good accuracy. Based on the observations

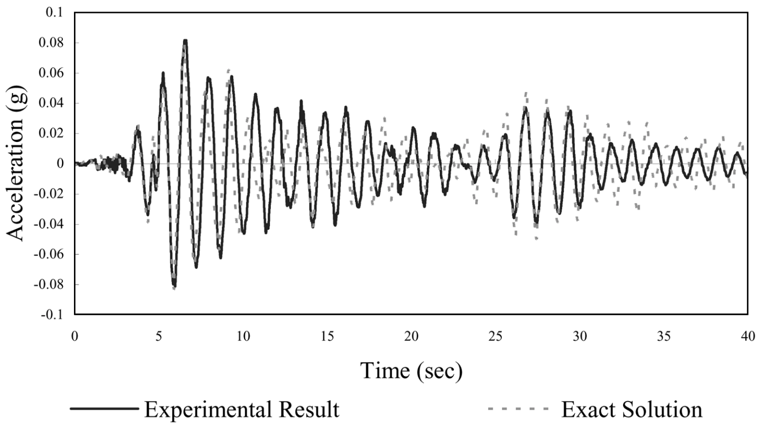

Fig. 12 Comparison of bearing acceleration between exact solution and experimental result under Chi-Chi earthquake (TCU129) of 0.289 g in PGA

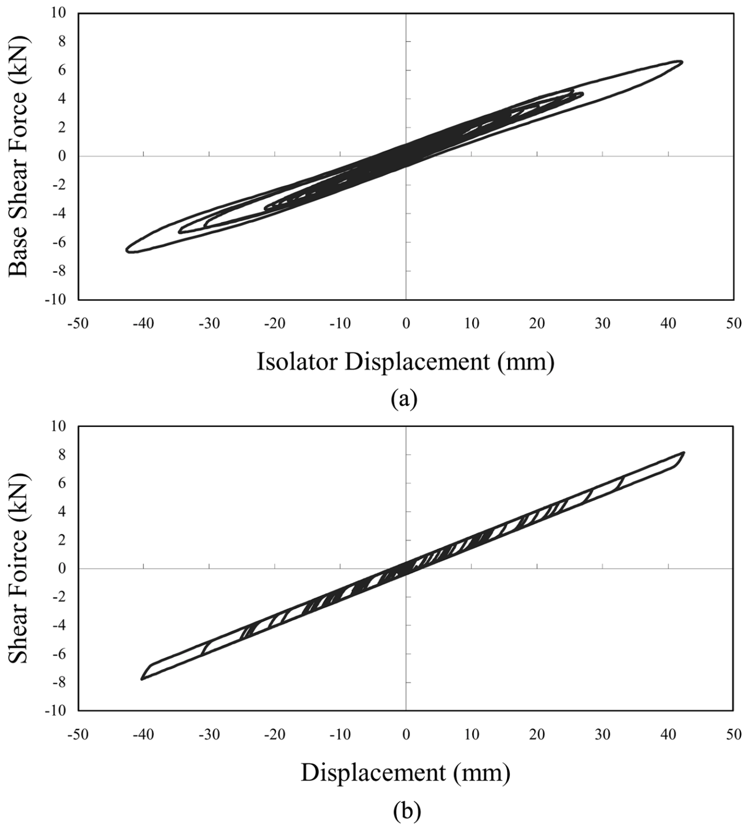

Fig. 13 Comparison of hysteresis loop between exact solution and experimental result under Chi-Chi earthquake (TCU129) of 0.289 g in PGA: (a) Experimental result; (b) Exact solution

aforementioned, it can be concluded that the exact solution can be given as a simple yet accurate method for engineering professions in preliminary design for elastomeric bearings.

7. Comparisons between exact solutions and numerical results from nonlinear analyses for VCFPS isolated structures

The comparisons between the exact solutions and the numerical results from the nonlinear finite element computer program are presented in this section (Tsai 1996). As shown in Fig. 14, a three-dimensional reinforced concrete building has been given as a numerical example. The building is 30.5 m in height, and the dimensions of the cross sections of columns and girders are 0.8 m × 0.8 m and 0.45 m × 0.8 m, respectively. The elastic modulus and Poisson's ratio of the building's construction material are 2.46×10^7 kN/m^2 and 0.2, respectively. The total weight of structure is 81207.18 kN. The fundamental period of the fixed-base structure in x and y direction are 1.025 sec and 1.079 sec, respectively. The fundamental period at the center of the concave sliding surface of the VCFPS is 2.5 sec, and the designed restoring force can bring the slider back to the center of the isolator when the isolator displacement is less than 0.8 m. The parameters μ_{min}, μ_{max} and α for Eq. (28) are 0.042, 0.102 and 1.903, respectively. The comparisons of the sliding displacement and the average hysteresis loop under the 1940 El Centro earthquake (Imperial Valley Station) between the exact solutions and results from the NSAT computer program are displayed in Figs. 15 and 16, respectively. It is shown from these two figures that the hysteresis behavior and the stiffness-softening phenomenon calculated from the exact solution are very close to that from the NSAT program.

In recent years, there have been significant studies on the seismic response of the base isolated structure under near-fault earthquakes. The long predominant periods and the pulse-like ground velocity can give the base isolator a significant relative displacement. Therefore, it is interest to validate whether the exact solution can predict such phenomenon or not. The comparisons of the sliding displacement and the average hysteresis loop under the Chi-Chi earthquake (TCU068 Station) between the exact solutions and results from the NSAT computer program are displayed in Figs. 17 and 18, respectively. The large displacement and the significant base shear force from the exact solution and the NSAT program are very correlated.

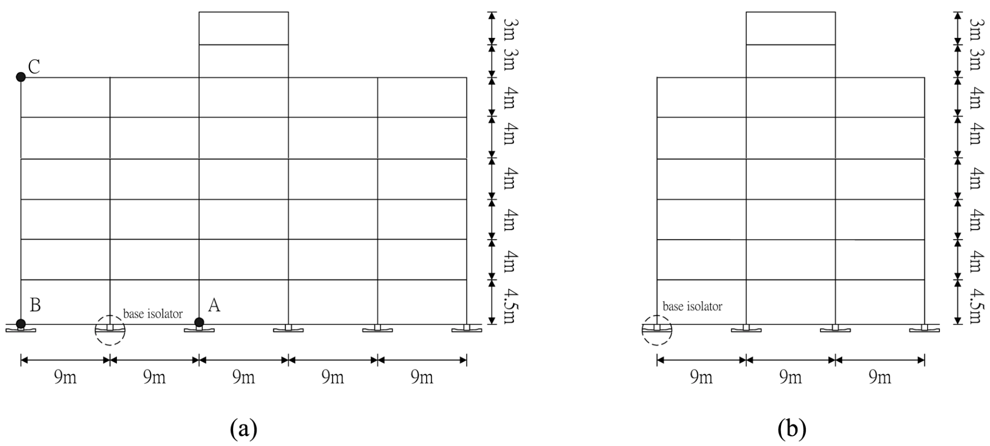

Fig. 14 A six-story reinforced concrete building: (a) Longitudinal direction; (b) Transverse direction

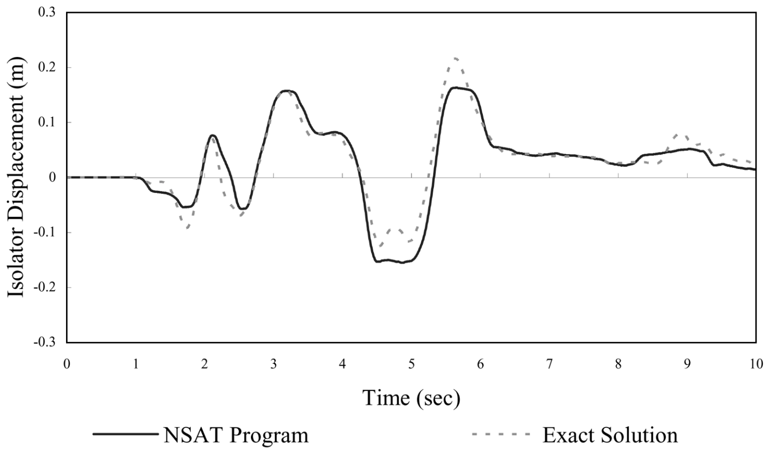

Fig. 15 Comparison of sliding displacement between exact solution and numerical result from nonlinear analysis during 1940 El Centro earthquake of 1.0 g

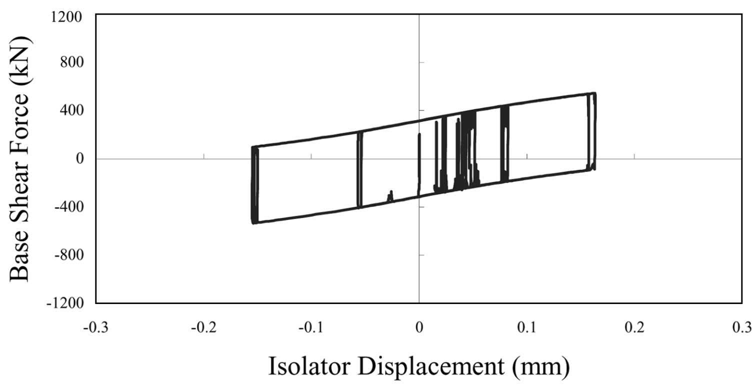

(a)

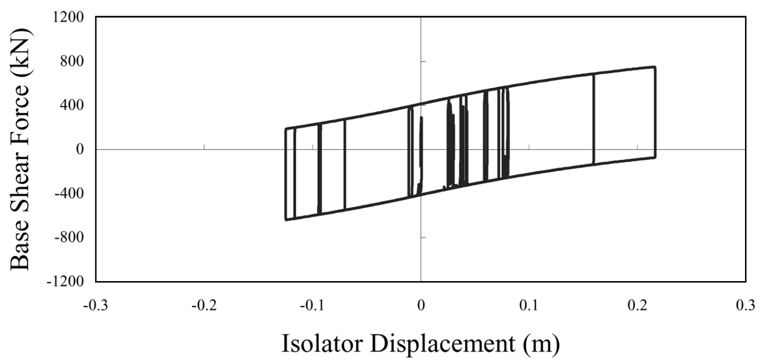

(b)

Fig. 16 Comparison of hysteresis loop between exact solution and numerical result from nonlinear analysis during 1940 El Centro earthquake of 1.0 g in PGA: (a) Numerical results from NSAT program; (b) Exact solution

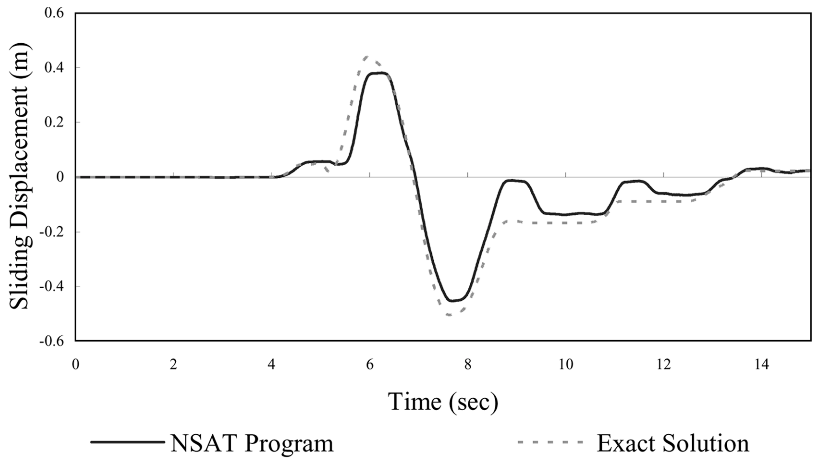

Fig. 17 Comparison of sliding displacement between exact solution and numerical result from nonlinear analysis during 1999 Chi-Chi earthquake of 0.511 g in PGA

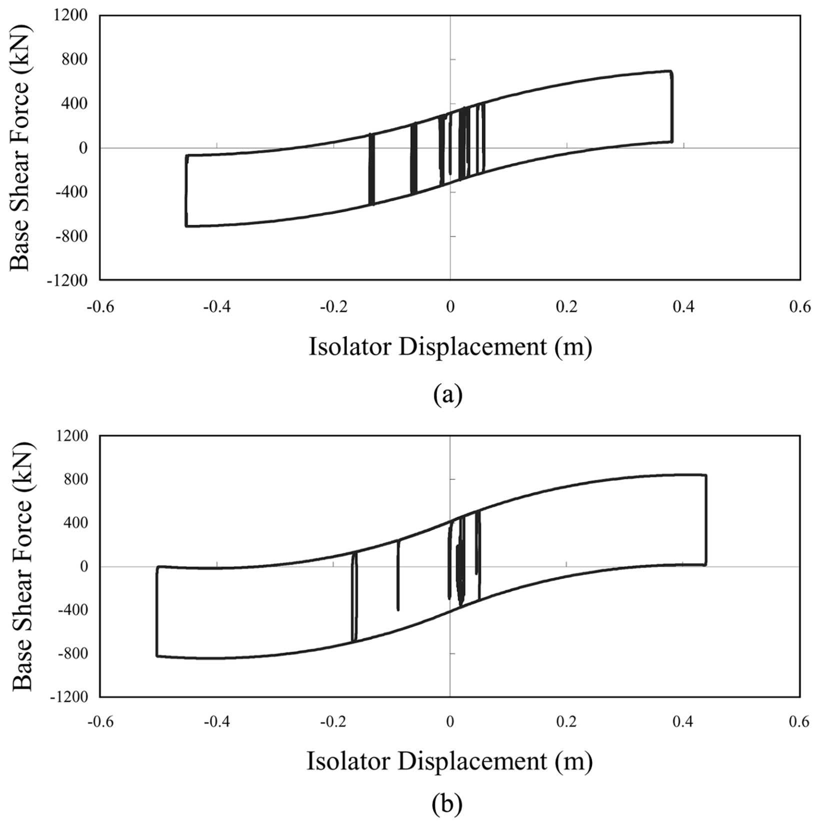

Fig. 18 Comparison of hysteresis loop between exact solution and numerical result from nonlinear analysis during 1999 Chi-Chi earthquake of 0.511 g in PGA: (a) Numerical results from NSAT program; (b) Exact solution

Table 1 Comparison of maximum bearing displacement of SRB under different earthquakes

	Analytical results	Experimental results
1940 El Centro (PGA=0.116 g)	0.031 m	0.036 m
1999 Chi-Chi (PGA=0.289 g)	0.043 m	0.042 m

Table 2 Comparison of maximum bearing acceleration of SRB under different earthquakes

	Analytical results	Experimental results
1940 El Centro (PGA=0.116 g)	0.0708 g	0.0686 g
1999 Chi-Chi (PGA=0.289 g)	0.0833 g	0.0817 g

Table 3 Comparison of maximum sliding displacement of VCFPS under different earthquakes

	Exact solution	NSAT program
1940 El Centro (PGA=1.0 g)	0.216 m	0.163 m
1999 Chi-Chi (PGA=0.511 g)	0.453 m	0.503 m

8. Conclusions

Exact formulations assuming rigid body response of a structure isolated with sliding-type and elastomeric-type base isolators have been derived in this study. The use of the proposed single degree-of-freedom exact solutions can save a large amount of calculation time with good accuracy. Comparisons between the exact solutions, experimental results and the numerical results from the nonlinear finite element computer program demonstrate the feasibility of the proposed concept. The displacement history, hysteresis behavior and the isolation period of the base isolator can be predicted accurately based on the observation of this study. Hence, the method proposed in this study can be adopted for engineering professions to determine the dimensions of bearings during the process of the preliminary design.

References

Al-Hussaini, T.M., Zayas, V.A. and Constantinou, M.C. (1994), “Seismic isolation of multi-story frame structures using spherical sliding isolation systems”, Technical Report, NCEER-94-0007.

Chen, B.J. (2003), “Characteristic and earthquake-proof benefits of rubber bearings”, Ph. D. Dissertation, Graduate Institute of Civil & Hydraulic Engineering, Feng-Chia University, Taichung, Taiwan, R. O. C..

Chopra, Anil K. (1995), *Dynamics of Structures, Theory and Applications to Earthquake Engineering*, Prentice-Hall, Inc.

Constantinou, M., Mokha, M. and Reinhorn, A. (1990), “Teflon bearings in base isolation. II: Modeling”, *J. Struct. Eng.*, ASCE, **116**(2), 455-474.

Nigam, N.C. and Jennings, P.C. (1968), “Digital calculations of response spectra from strong-motion earthquake records”, Earthquake Engineering Research Laboratory, California Institute of Technology, EERL, Pasadena, CA.

Nigam, N.C. and Jennings, P.C. (1969), “Calculation of response spectra from strong motion earthquake records”, *Bulletin of the Seismological Society of America*, **59**, 909-922.

Tsai, C.S. (1995), “Seismic behavior of buildings with FPS isolators”, *Second Congress on Computing in Civil Engineering*, ASCE, Atlanta, GA, 1203-1211.

Tsai, C.S. (1996), “Nonlinear stress analysis techniques-NSAT”, Feng-Chia University, Department of Civil Engineering, Taichung, Taiwan, R. O. C..

Tsai, C.S. (1997), “Finite element formulations for friction pendulum seismic isolation bearings”, *Int. J. Numer. Meth. Eng.*, **40**, 29-49.

Tsai, C.S., Chen, B.J. and Chiang, T.C. (2002), “Reasonable lateral force distributions on isolated structures”, *2002 ASME Pressure Vessels and Piping Conf.*, Vancouver, Canada, 2, Edited by S.C. Lu, 229-236.

Tsai, C.S., Chen, B.J. and Chiang, T.C. (2003a), “Experimental and computational verification of reasonable formulae for based-isolated structures”, *Earthq. Eng. Struct. Dyn.*, **32**, 1389-1406.

Tsai, C.S., Chiang, T.C. and Chen, B.J. (2003b), “Finite element formulations and theoretical study for variable curvature friction pendulum system”, *Eng. Struct.*, **25**, 1719-1730.

Tsai, C.S., Chiang, T.C., Chen, B.J. and Lin, S.B. (2003c), “An advanced analytical model for high damping rubber bearings”, *Earthq. Eng. Struct. Dyn.*, **32**, 1373-1387.

Zayas, Victor A., Low, Stanley S. and Mahin, Stephen A. (1987), “The FPS earthquake resisting system experimental report”, Technical Report, UBC/EERC-87/01.